Solid State Communications 254 (2017) 42–47

Contents lists available at ScienceDirect

Solid State Communications

journal homepage: www.elsevier.com/locate/ssc

Communication

Sensitivity of helical edge states to line substitutional magnetic doping in zigzag silicene nanoribbons

Xiongwen Chen[a,*], Zhengang Shi[a], Baoju Chen[a], Shaohua Xiang[a], Guanghui Zhou[b,*]

[a] Department of Mechanical engineering and Photoelectric Physics, Huaihua University, Huaihua, 418008 China
[b] Key Laboratory for Low-Dimensional Structures and Quantum Manipulation, Synergetic Innovation Center for Quantum Effects and Applications, Hunan Normal University, Changsha, 410081 China

ARTICLE INFO

Communicated by F. Peeters

Keywords:
Zigzag silicene nanoribbons
Line magnetic doping
Spin-resolved semiconductor
Pure spin current

ABSTRACT

Using the tight-binding model, we investigate the sensitivity of helical edge states to a line magnetic doping in the zigzag silicene nanoribbons (ZSiNRs). We find that it is only sensitive to the doping in the odd-numbered line of the edge region. Moreover, a phase transition from the topological insulator to the spin-resolved semiconductor can be induced by the magnetic doping only in the first line. Accordingly, importantly, the pure spin-up and -down currents come into being in two adjacent energy regions around the Fermi level. Therefore, a spin-current conversion can be realized in the ZSiNRs, which may be useful to the design of controllable spintronic device.

1. Introduction

Silicene, a slightly buckled monolayer of hexagonal silicon lattice, has attracted considerable attention recently based on its compatibility with conventional Si-based semiconductor industry [1,2]. Recently, silicene nanoribbons (SiNRs) have been fabricated on the silver surface [3,4], which provides a basic component to the silicene-based electronics. Just like the graphene nanoribbons (GNRs) [5], SiNRs can also be classified into two types of armchair-edge SiNRs (ASiNRs) and zigzag-edge SiNRs (ZSiNRs) according to the configuration of edge atoms. However, a rather strong spin–orbit interaction λ_{SO} = 3.9 meV makes a perfect ZSiNR to become a topological insulator [6], which possesses a novel electronic structure characterized by a full insulating bulk and two metallic edges. The metallic edges are determined by the helical gapless edge subband, which are topologically protected by the time-reversal symmetry [7,8]. Due to the buckled structure of silicene, the structural symmetry can be easily destroyed by a perpendicular electric field [9,10], which produces two different on-site potentials at the *A* and *B* sublattice sites (see Fig. 1). This drives a phase transition from a topological insulator to a band insulator in the nonmagnetic ZSiNRs [10]. Additionally, a local exchange field in one edge region of ZSiNRs can induce a spin-polarized current in the opposite edge since the local time-reversal symmetry is broken in the chosen edge and still robust against the exchange field in the opposite edge [11]. By employing sufficient impurities and defects, the half-metal [12,13] and the spin-polarized transport [14,15] can also be realized even without external fields. Motivated by the above results, a fundamental question arises. Which positions are appropriate to be substituted by impurities or covered by local external field for the aim of modulating the electron structure in a ZSiNR. This question, to our knowledge, has not been answered.

In this work, we investigate the influence of a line magnetic doping in different positions to the electron structure of a ZSiNR. As depicted in Fig. 1, a *N*-ZSiNR is composed of *N* transverse zigzag atomic chains, and every chain includes two lines. We assume that Si atoms at line ℓ are all substituted by the magnetic impurities (red squares), which can induce a local exchange magnetic field at the positions of the dopants [16,17]. Using the tight-binding model and Green's function (GF) approach, we calculate the band structure and the local density of states (LDOS) in a *N*-ZSiNR. It is shown that the helical edge subband is highly sensitive to the magnetic doping in the odd-numbered line of edge region. However, it is almost insensitive to the doping in the even-numbered line. In particular, when the dopants locate at the edge line (ℓ=1), an obvious gap is opened in the edge subband. Interestingly, two gaps in the spin-up and -down band structures do not coincide with each other and are separated by the Fermi level, which induces a phase transition from the topological insulator to the spin-resolved semiconductor. Accordingly, a conversion of the spin-down and -up currents can be realized in the ZSiNRs, which may be useful to the design of controllable spintronic device.

* Corresponding authors.
E-mail addresses: hnsxw617@163.com.cn (X. Chen), ghzhou@hunnu.edu.cn (G. Zhou).

http://dx.doi.org/10.1016/j.ssc.2016.12.019
Received 13 October 2016; Received in revised form 22 December 2016; Accepted 23 December 2016
Available online 25 December 2016

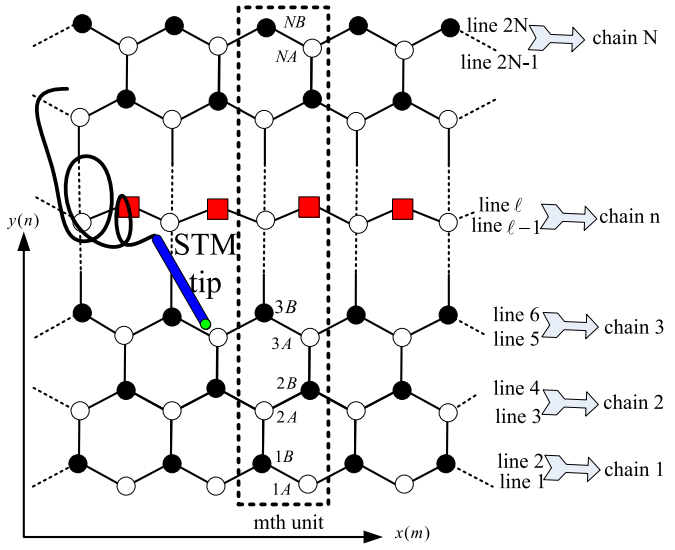

Fig. 1. (Color online) Top view of a *N*-ZSiNR with a line substitutional magnetic doping, where the (black) solid and hole spheres indicate silicon atoms of two subplanes, respectively, and the (red) squares are the magnetic dopants at line ℓ. The (black) dashed line rectangle represents the *m*th unit along the longitudinal *x*-direction.

2. Hamiltonian and method

The structure of a *N*-ZSiNR with a line of magnetic substituted atoms is illustrated in Fig. 1. The Hamiltonian can be described by a four band second-nearest-neighbor tight-binding model [18,19],

$$H = -t\sum_{\langle i,j\rangle,\alpha} c^{\dagger}_{i,\alpha}c_{j,\alpha} + i\frac{\lambda_{SO}}{3\sqrt{3}}\sum_{\langle\langle i,j\rangle\rangle,\alpha\beta}\vartheta_{ij}c^{\dagger}_{i,\alpha}\sigma^{z}_{\alpha\beta}c_{j,\beta} + i\frac{2\lambda_R}{3}\sum_{\langle\langle i,j\rangle\rangle,\alpha\beta}\mu_{ij}c^{\dagger}_{i,\alpha}(\sigma\times\mathbf{d}_{ij})^{z}_{\alpha\beta}c_{j,\beta} + \sum_{\alpha}\alpha M c^{\dagger}_{\ell,\eta,\alpha}c_{\ell,\eta,\alpha}, \quad (1)$$

where $c^{\dagger}_{i,\alpha}$ ($c_{i,\alpha}$) is the creation (annihilation) operator of an electron at site $i=(m,\eta)$ with $\eta = nA,\ nB$, $\alpha = +/-1$ denotes spin-up/down, $\boldsymbol{\sigma}=(\sigma_x,\sigma_y,\sigma_z)$ is the Pauli operator, and $\langle i,j\rangle$ and $\langle\langle i,j\rangle\rangle$ run over all the nearest and next-nearest neighbor sites, respectively. The lattice constant of silicene is $a_0 = 3.86$ Å. The first term in (1) is the nearest-neighbor hopping with energy t=1.6 eV, the second term describes the effective spin–orbit interaction with strength $\lambda_{SO} = 3.9$ meV, which concerns the nearest-neighbor bonds $\mathbf{d}_i$ and $\mathbf{d}_j$ connecting an atom to its next-nearest-neighbor $\mathbf{d}_{ij}$. The coefficient ϑ_{ij} takes the value $+1/-1$ if the next-nearest neighboring hopping is anticlockwise/clockwise with respect to the positive z-axis. The third term with $\lambda_R = 0.7$ meV describes the Rashba interaction generated by the non-coplanar two sublattices. The last term denotes the magnetic doping in line ℓ with the electronic creation (annihilation) operator $c^{\dagger}_{\ell,\alpha}$ ($c_{\ell,\alpha}$), where an exchange interaction with strength M is induced by the magnetic impurities [16,17].

The band structure $E(k)$ can be obtained by solving the Schröinger equation

$$H|\Psi\rangle = E(k)|\Psi\rangle, \quad (2)$$

where the wavefunction can be expressed in the form of $|\Psi\rangle = \sum_m\sum_{\eta,\alpha}\psi^{\alpha}_{m,\eta}|m,\eta,\alpha\rangle$, in which $\psi^{\alpha}_{m,\eta} = \langle m,\eta,\alpha|\Psi\rangle$ is the local

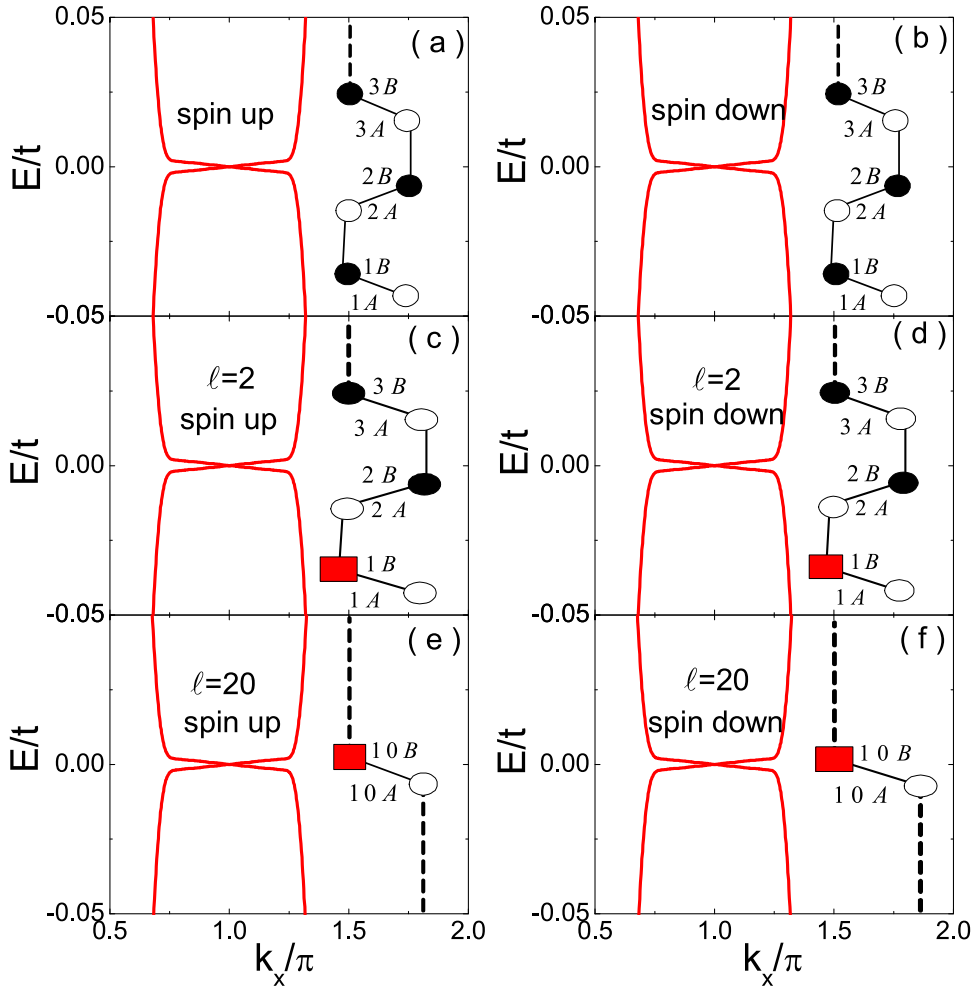

Fig. 2. (Color online) Edge subband $E(k)$ for 21-ZSiNR. (a, b) are for the perfect case. Other figures are for a line magnetic doping at the even-numbered line: (c, d) ℓ=2 and (e, f) ℓ=20.

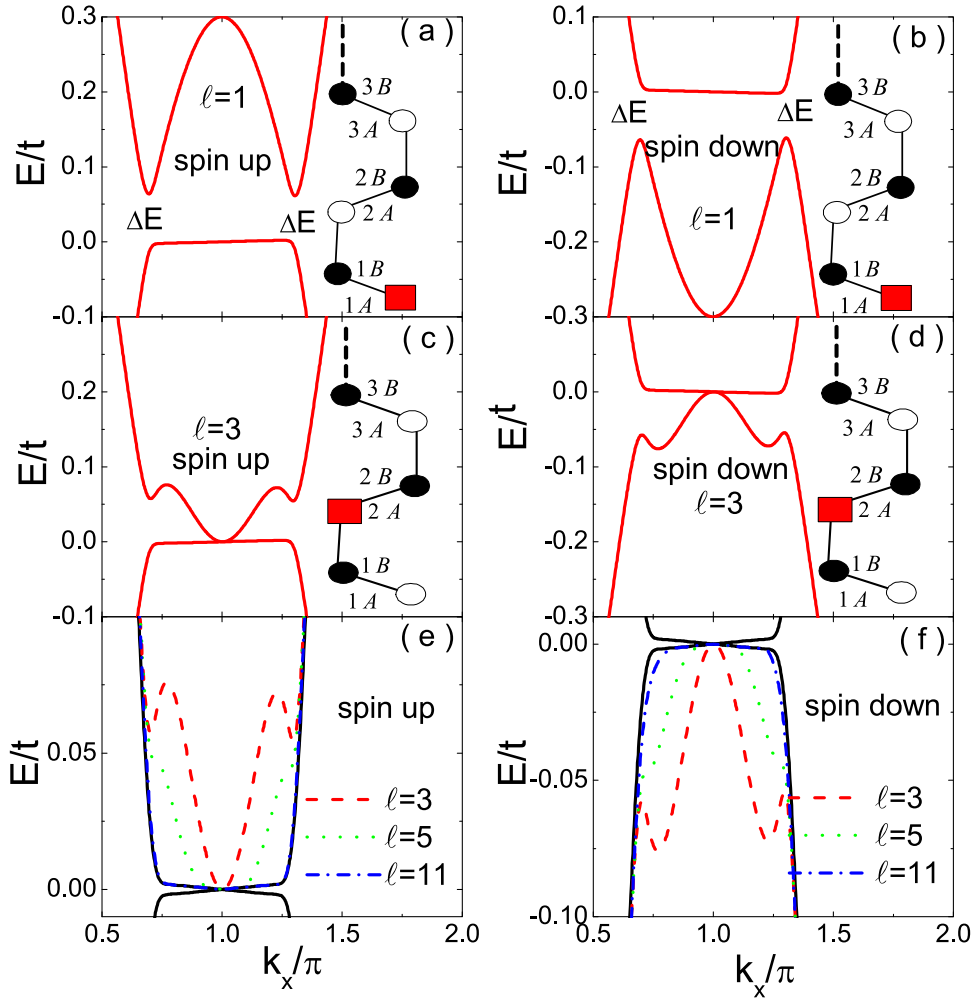

Fig. 3. (Color online) Edge subband $E(k)$ of 21-ZSiNR with a line magnetic doping at the odd-numbered line: (a, b) for ℓ=1, (c, d) for ℓ=3, and (e, f) for comparison with different ℓ.

wavefunction component at site (m, η) with $|m, \eta, \alpha\rangle = c^{\dagger}_{i,\alpha}|vacuum\rangle$ and $i = (m, \eta)$. For a N-ZSiNR with finite width in the y-direction as shown in Fig. 1, the Hamiltonian exhibits a translational symmetry along the x-direction. The local wavefunction component can be finally rewritten in form of $\psi^{\alpha}_{m,\eta} = f^{\alpha}_{\eta} e^{ikx_{m,\eta}}$, where k is the wavevector along the x-direction, the x-coordinate $x_{m,\eta}$ is defined by the equations $x_{m,1B} = x_{m,2A} = x_{m,3B} = \cdots \equiv x_m$. The coefficient f^{α}_{η} is a y-direction site coefficient at site (m, η), where a periodical boundary condition $f^{\alpha}_{0B} = f^{\alpha}_{(N+1)A}$ is satisfied (see Fig. 1). In the following calculation, the exchange interaction $M = 0.3t$ is taken as a theoretical analysis but its value is not unessential to our results. Additionally, the weak Rashba interaction is neglected because it does not qualitatively affect our results.

To obtain the LDOS at various sites in the N-ZSiNR, we introduce the retarded GF with a form of $4N \times 4N$ spin-resolved matrix $g^r(E) = 1/[E + i\delta^+)I_0 - H]$, where I_0 is a unit matrix and δ^+ is a positive infinitesimal. Then the LDOS for spin-α electron at site (m, η) can be calculated through a formula

$$LDOS(E) = -\frac{1}{\pi}\Im[g^r_{m,\eta,\alpha}(E)], \tag{3}$$

where $g^r_{m,\eta,\alpha}(E)$ is the matrix element of $g^r(E)$ at site (m, η). This electronic local distribution can be observed experimentally by the spatially high-resolution scanning tunneling microscopy (STM) [3,4]. We theoretically simulate it as follows.

We fix the Fermi level of the ZSiNR at zero value, i.e., ϵ_F=0. Accordingly, the STM tip, its end atom, and the ZSiNR construct a two-terminal electron transport system (see Fig. 1). When the potential of STM tip $u > 0$ is taken, electrons in the tip transport from its end atom to site (m, η) of the ZSiNR, and propagate along different chains. Therefore, the spin-resolved STM current can be expressed by

$$I_{\eta,\alpha} = \frac{e}{h}\int_{\epsilon_F}^{u} dE[f_2(E-u) - f_1(E-\epsilon_F)]T_{\eta,\alpha}(E), \tag{4}$$

where $f_{1(2)}(E)$ is the Fermi–Dirac distribution function for the ZSiNR (tip). The function $T_{\eta,\alpha}(E)$ is the electron transmission, which can be calculated by means of the nonequilibrium GF approach [20–22].

3. Results and discussion

Fig. 2 shows the helical edge subband $E(k)$ with magnetic doping at different even-numbered lines in 21-ZSiNR. For comparison, in Figs. 2(a) and (b), we show the spin-up and -down $E(k)$ in the perfect case (without defect), respectively. When the dopants locate at sites 1B of line 2 in the edge chain 1 [Figs. 2(c) and (d)] and 10B of line 20 in central chain 10 [Fig. 2(e) and (f)], the shapes of $E(k)$ are nearly identical to that in the perfect case. Moreover, there is no difference between the cases of the spin-up and -down subband. This implies that the helical gapless subband is highly insensitive to the magnetic substitutions at the even-numbered lines, despite breaking the time-reversal symmetry of this system by introducing the magnetic doping.

However, the helical edge subband $E(k)$ is highly sensitive to the magnetic doping in the odd-numbered line of the edge region, which is displayed in Fig. 3. When the dopants locate at site 1A of line 1, the conduction and valence inverse in the spin-up and -down edge subbands [Figs. 3(a) and (b)], respectively. This difference originates

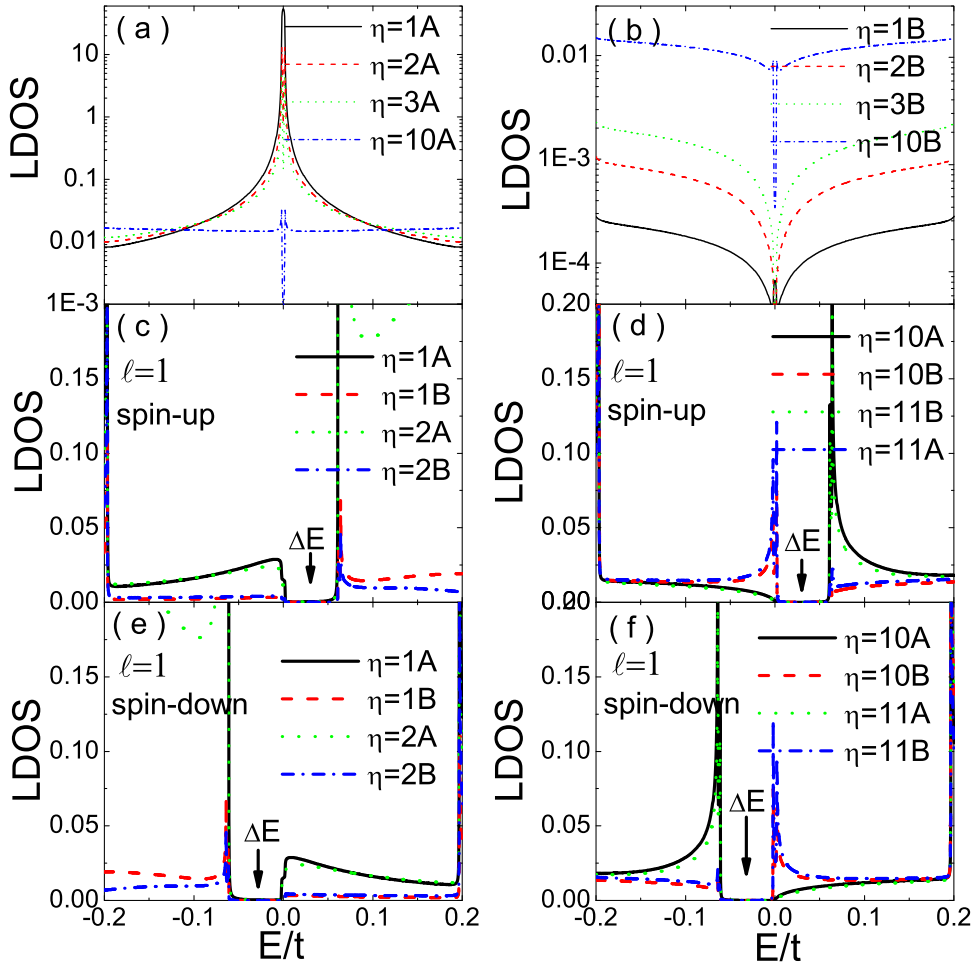

Fig. 4. (Color online) Local density of states *LDOS*(*E*) at different sites in 21-ZSiNR with magnetic doping at line 1, where (a) and (b) are perfect case as a comparison.

from the fact that the magnetic doping provides the different exchange potentials M and $-M$ to the spin-up and -down electrons, respectively. Importantly, two gaps in the spin-up and -down band structures do not coincide with each other and are separated by the Fermi level. Resultantly, a phase transition from the topological insulator to the spin-resolved semiconductor is realized. Moreover, as a whole, the ZSiNR displays a metallic (gapless semiconducting) property because the valence of spin-up edge subband and the conduction of spin-down edge subband meet at the Fermi level. When the dopants locate at site of the other odd-numbered line, such as line 3 [see Figs. 3(c) and (d)], the gap of the edge subband disappears but its helical property is obviously destroyed. Moreover, Figs. 3(e) and (f) show that the influence of the line doping becomes weaker and weaker with the variation of its location from lines 3 to 5, 11. When the dopants locate at line 11 in the center of the ribbon, the edge subband [(blue) solid-dashed line] coincides hardly with the perfect case [the (black) solid line]. This phenomenon manifests that the line doping in the center region of ZSiNR is invalid to modulate the band structure. The sensitivity can be explicated by the LDOS in a ZSiNR as follows.

Fig. 4 shows the LDOS at different sites in 21-ZSiNR with and without magnetic doping in line ℓ=1. In the case of without doping, the LDOS exhibits a sharp peak around the Fermi level at the sites in the odd-numbered lines such as 1A of line 1, 2A of line 3, and 3A of line 5, as shown in Fig. 4(a). But the peak height becomes lower and lower until it disappears [see (blue) dash-dot line in Fig. 4(a)] when the doping location varies from the edge to the center region of the ribbon. In contrast, the center peaks are always absent and replaced by dips at sites in the even-numbered lines such as site 1B of line 2, 2B of line 4, 3B of line 6 and 10B of line 20 [see Fig. 4(b)]. This implies that the helical edge subband is only occupied by electrons at the odd-numbered lines of the edge region. Therefore, only the dopants located at the odd-numbered line of the edge region can affect the helical edge states in a ZSiNR, which is consistent with Figs. 2 and 3. Importantly, when the dopants locate at line 1, the LDOS has a zero value with a gap of width ΔE. Moreover, the two gaps in the spin-up [Figs. 4(c) and (d)] and -down [Figs. 4(e) and (f)] LDOS do not coincide with each other and are separated by the Fermi level. Therefore, we conclude that the spin-up and -down currents in two adjacent energy regions can be induced by the magnetic doping at line 1, which is analyzed by simulating the STM current [3,4] as follows.

In Fig. 5 we show the spin-resolved STM current $I_{\eta,\alpha}(u)$ through site (m, η) in 21-ZSiNR. Compared to the perfect zigzag-edge (ZGNRs) [22], an opposite odd–even rule exists in ZSiNRs displayed in Figs. 5(a) and (c). For example, when the tip contacts to site (m, 1A) in line 1, the current $I_{\eta,\alpha}$ rises rapidly although a very small potential u (>0), approaching zero value, is given in STM tip [see the (black) solid line in Fig. 5(a)]. This behavior also appears but becomes weaker at other sites of odd-numbered lines in the edge region such as sites 2A of line 3 [see the (green) dot line in Fig. 5(a)]. However, it does not appear at sites of even-numbered lines such as sites 1B of line 2 [(red) dashed line] and 2B of line 4 [(blue) dash-dot line]. This rule is opposite in the perfect ZGNRs [22]. This difference between ZGNRs and ZSiNRs originates from the fact that the edge subband is flat in ZGNRs while it is helical in ZSiNRs. Therefore, the electron state [LDOS(E) in Fig. 4(a)] at the edge is nonlocalized in ZSiNRs while it is localized in ZGNRs. This odd–even rule provides a chance to verify that the helical edge subband is only occupied by electrons in the odd-numbered lines of edge region. Importantly, when a line magnetic doping is in line 1,

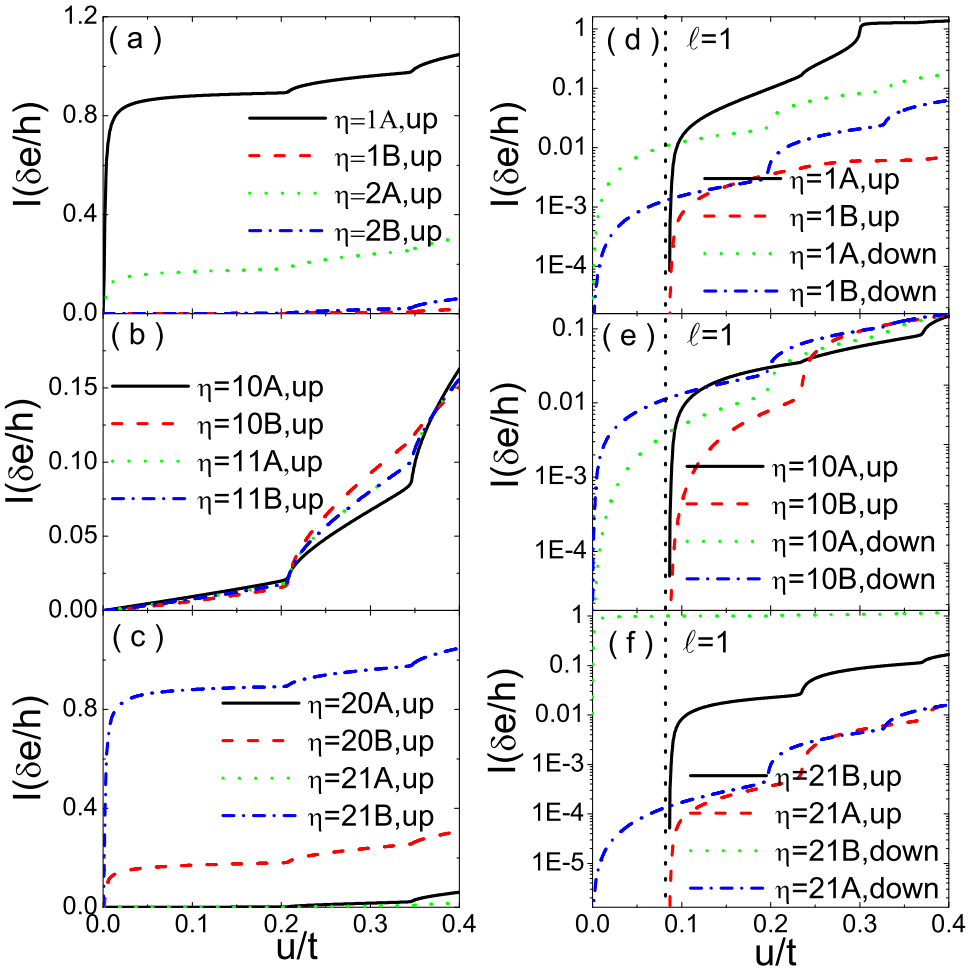

Fig. 5. (Color online) Scanning tunneling microscopy current $I(u)$ at different sites in 21-ZSiNR. The left panel is for the perfect case and the right panel is for the case of magnetic doping at line ℓ=1. The parameter $\delta = 1.0 \times 10^{-4}$ is taken.

we can see easily that two pure spin STM currents occur in all sites of ZSiNRs. As shown in Figs. 5(d–f), when the potential of STM tip $0 < u < u_c$ (threshold potential for the occurrence of current) is taken, the current $I_{\eta,\downarrow}$ appears and the current $I_{\eta,\uparrow}$ disappears. Accordingly, it is reasonable to deduce that when the potential $-u_c < u < 0$ is taken, the current $I_{\eta,\uparrow}$ appears and the current $I_{\eta,\downarrow}$ disappears (no show in here) based on the rule of LDOS in Fig. 4. How to generate spin-polarized currents in the low-dimensional systems is one of the main challenges in the field of spintronics. Therefore, our result may be helpful for the design of the silicene-based spintronic device.

4. Conclusions

In conclusion, we have investigated the sensitivity of helical edge state to the line magnetic doping in ZSiNRs by employing the tight-binding model. It has shown that the helical edge subband is highly sensitive to the line doping in the odd-numbered line of the edge region, while it is insensitive to the existence of the line doping in the even-numbered line. Also, it is also insensitive to the line doping in the center region, no matter whether the doping is in the odd- or even-numbered line. Interestingly, a transition from the topological insulator to the spin-resolved semiconductor occurs when the line magnetic doping locates at line 1. Therefore, the pure spin-up and -down electronic transports realize in ZSiNRs and they distribute in two adjacent energy regions, which should be useful to spintronic device. Additionally, it is worth mentioning that the helical edge subband can be manipulated by introducing photo-irradiation [23,24] based on the Haldane term [25]. When the photoinduced topological phase becomes strong enough [23], the line magnetic impurities only destroy the helical edge mode of its corresponding edge. Therefore, a spin-polarized current is observed in other edge (no defect), which is very similar to the results of Ref. [16] based on the Kane–Mele Hamiltonian in a honeycomb lattice [26]. At this case, the spin-resolved semiconductor in our results disappears once the topological phase becomes strong enough.

Acknowledgments

We thank Prof. Dr. Zhongshui Ma in School of Physics of Peking University for insightful discussions. This work was supported by the National Natural Science Foundation of China under Grant nos. 11347009, 11174100 and 11274108, and the Hunan Provincial Natural Science Foundation under Grant no. 14JJ2130.

References

[1] A. Kara, H. Enriquez, A.P. Seitsonen, L.C.L.Y. Voone, S. Vizzini, B. Aufray, H. Oughaddou, Surf. Sci. Rep. 67 (2012) 1.
[2] L.C.L.Y. Voon, J. Zhu, U. Schwingenschlögl, Appl. Phys. Rev. 3 (2016) 040802.
[3] B. Aufray, A. Kara, S. Vizzini, H. Oughaddou, C. Léandri, B. Ealet, G.L. Lay, Appl. Phys. Lett. 96 (2010) 183102.
[4] P.D. Padova, C. Quaresima, C. Ottaviani, P.M. Sheverdyaeva, P. Moras, C. Carbone, D. Topwal, B. Olivieri, A. Kara, H. Oughaddou, B. Aufray, G.L. Lay, Appl. Phys. Lett. 96 (2010) 261905.
[5] K. Nakada, M. Fujita, G. Dresselhaus, M.S. Dresselhaus, Phys. Rev. B 54 (1996) 17954.
[6] M. Ezawa, N. Nagaosa, Phys. Rev. B 88 (2013) 121401(R).
[7] C.L. Kane, E.J. Mele, Phys. Rev. Lett. 95 (2005) 146802.
[8] W.-F. Tsai, C.-Y. Huang, T.-R. Chang, H. Lin, H.-T. Jeng, A. Bansil, Nat. Commun.

4 (2013) 1500.
[9] N.D. Drummond, V. Zólyomi, V.I. Fal'ko, Phys. Rev. B 85 (2012) 075423.
[10] M. Ezawa, New J. Phys. 14 (2012) 033003.
[11] X.-T. An, Y.-Y. Zhang, J.-J. Liu, S.-S. Li, New J. Phys. 14 (2012) 083039.
[12] Y. Ding, Y. Wang, Appl. Phys. Lett. 102 (2013) 143115.
[13] F.-B. Zheng, C.-W. Zhang, P.-J. Wang, S.-S. Li, J. Appl. Phys. 113 (2013) 154302.
[14] N.B. Le, T.D. Huan, L.M. Woods, Phys. Rev. Appl. 1 (2014) 054002.
[15] M. Yang, D.-H. Chen, R.-Q. Wang, Y.-K. Bai, Phys. Lett. A 379 (2015) 396.
[16] Q. Liu, C.-X. Liu, C. Xu, X.-L. Qi, S.-C. Zhang, Phys. Rev. Lett. 102 (2009) 156603.
[17] X.-T. An, Y.-Y. Zhang, J.-J. Liu, S.-S. Li, J. Phys.: Condens. Matter 24 (2012) 505602.
[18] C.-C. Liu, W. Feng, Y. Yao, Phys. Rev. Lett. 107 (2011) 076802.
[19] C.-C. Liu, H. Jiang, Y. Yao, Phys. Rev. B 84 (2011) 195430.
[20] T. Fukuda, H. Oymak, J. Hong, J. Phys.: Condens. Matter 20 (2008) 055207.
[21] N.M.R. Peres, S.-W. Tsai, J.E. Santos, R.M. Ribeir, Phys. Rev. B 79 (2009) 155442.
[22] X. Chen, H. Wan, K. Song, D. Tang, G. Zhou, Appl. Phys. Lett. 98 (2011) 263103.
[23] M. Ezawa, Phys. Rev. Lett. 110 (2013) 026603.
[24] M. Ezawa, Appl. Phys. Lett. 102 (2013) 172103.
[25] F.D.M. Haldane, Phys. Rev. Lett. 61 (1988) 2015.
[26] C.L. Kane, E.J. Mele, Phys. Rev. Lett. 95 (2005) 226801.